Optimal charging of a quantum battery

by

Quirijn van Hattem

to obtain the degree of Bachelor of Science at the Delft University of Technology, to be defended publicly on Monday June 26, 2023.

Student number:	5113792	
Project duration:	Februari 1, 2023 – Juni 26, 2023	
Thesis committee:	Dr. M. Blaauboer,	TU Delft, supervisor
	Dr. P. Visser,	TU Delft, supervisor
	Dr. S. Eijt,	TU Delft
	Dr. W. Groenevelt,	TU Delft

An electronic version of this thesis is available at `http://repository.tudelft.nl/`.

TU Delft

Abstract

When delving into the realm of the smallest systems in nature, quantum mechanics is required to describe the time evolution of these systems. The storage of energy in such systems is achieved by means of so-called quantum batteries. This thesis investigates optimal charging for two types of quantum batteries, clarifying the role of entanglement in the process.

Firstly, the central-spin battery (CS-battery) is studied, where N_C number of 1/2-spin particles serve as the charger, coupled to N_B number of 1/2-spin particles that serve as the battery. Analytical solutions are presented for special cases in which the energy stored in the battery, denoted as E_B, reaches the maximum energy capacity C_{E_B}, as well as scenarios where E_B never reaches C_{E_B}. Numerical simulations of the time evolution are used for $N_B > 2$ to demonstrate that E_B does not reach C_{E_B} within a time period of $t < \pi^2$.

Subsequently, I introduce a novel model: the central-spin transmitter battery (CST-battery), in which the battery and charger particles are indirectly coupled via one 1/2-spin particle, which I called the transmitter. Two setups of the CST-battery are investigated: constant exchange coupling, where the coupling between both sides of the transmitter remains fixed, and varying exchange coupling, where the coupling between both sides of the transmitter changes. For constant exchange coupling, numerical simulations are used to show that E_B does not reach C_{E_B} within a time period of $t < \pi^2$. In the case of varying exchange coupling, it is demonstrated that by enabling or disabling the exchange coupling between the charger-transmitter and the transmitter-battery at precise moments, the mathematical representation of the CST-battery simplifies to that of a CS-battery with $N_B = 1$. This simplified scenario can be solved analytically. By following this approach, it is possible to fully charge the battery in the CST-battery system for arbitrary $N_C \geq N_B$, within a time period of $t < \pi^2$. The power of the CST-battery scales as $P \sim \frac{N_B}{\pi^2}$, as N_B approaches infinity.

Contents

Chapter 1

Introduction

In everyday life, the operation of big systems, such as steam engines and refrigerators, can be described by the laws of classical thermodynamics. Nowadays, there is a rapid development in creating complex technological systems which are getting smaller and smaller, like microchips for example. Eventually one will reach the scale where quantum mechanics is dominant, and where these complex systems cannot be described by classical thermodynamics anymore. This is where the theory of quantum thermodynamics comes into play. This theory investigates how concepts as energy, work and temperature can be transferred between quantum systems, where fluctuations and randomness are fundamentally unavoidable. In *Millen 2016* the perspectives on quantum thermodynamics and quantum machines are discussed [7, 8]. Recently, the study of quantum heat engines and refrigeration, energy storage and transfer in quantum-mechanical systems has gained significant interest. These systems, which can be used to store and extract energy, are so called "quantum batteries".

Entanglement is a primary feature in quantum mechanics. In a mathematical sense, two particles are entangled, if the quantum state of each particle cannot be described independently. To provide more clarity about this mathematical definition, a comparison is made between classical charging of a normal battery and charging of a quantum battery, where entanglement arises. In Figure 1.1, the classical charging process is depicted. The energy storage device on the left is called the charger and the energy storage device on the right is called the battery. From left to right, one can observe the battery transitioning from empty (red) to half-full (yellow), and eventually to a fully charged (green) state. During the charging process, the battery can be described independently (empty, half-full and full, etc.).

1

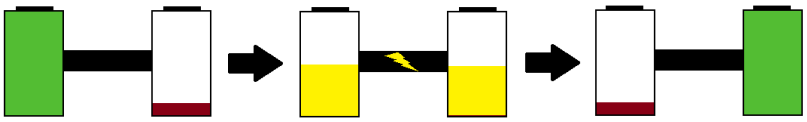

Figure 1.1: Classical charging of a battery. The energy storage device on the left is called the charger and the energy storage device on the right is called the battery. From left to right, one can observe the battery transitioning from empty (red) to half-full (yellow), and eventually to a fully charged (green) state. During the charging process, the states of the charger and battery can be described independently.

In Figure 1.2, the quantum charging process is depicted. Two spin particles are used for energy storage. The left spin particle is called the charger, and the right spin particle is called the battery. A spin particle can only be in spin up (full) or spin down (empty), not something in between. From left to right, one can observe that the battery is transitioning from empty to a superposition of empty and full, and eventually to a fully charged state. Being in a superposition of full and empty, the energy state of the battery cannot be described independently. The charger and battery are entangled.

There are many recent investigations of quantum batteries, [1, 3, 10]. It is shown that using entangling processes in an array of qubits can achieve a higher power than local operations, and entanglement generation benefits the speedup of work extraction. This is an advantage that arises when making use of these quantum properties. In *Peng 2021* and *Liu 2021* this advantage of charging power and work extraction is further investigated for the so-called central-spin battery, [6, 9].

In this thesis the role of entanglement and the optimal charging of a the central-spin battery is studied. Two types of batteries are investigated. First, the charging process of a central-spin quantum battery (CS-battery) is studied, where spin particles considered as the battery are directly coupled to spin particles considered as the charger. An illustration of this system is given in Figure 2.1. Following that, I have devised a pioneering model where an additional spin-particle, referred to

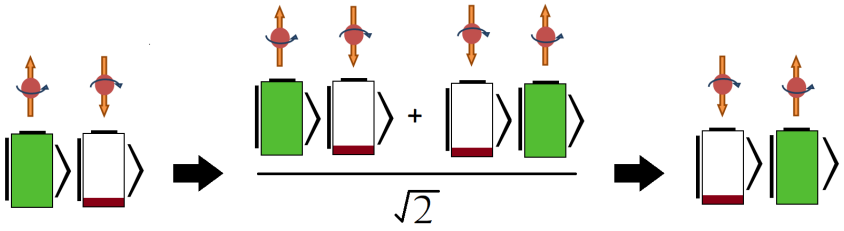

Figure 1.2: Quantum charging of a quantum battery. The left spin particle is called the charger and the right particle is called the battery. From left to right, one can observe that the battery is transitioning from empty to a superposition of empty and full, and eventually to a fully charged state. In the second step, the particles are entangled, the energy state of the battery and charger cannot be described independently.

as a transmitter, is positioned between the battery and the charger, creating what I call a CST-battery. This arrangement ensures that the battery and charger are solely connected through the transmitter. An illustration of this system is given in Figure 2.2. Also, the influence of modifying the exchange coupling in the CST-battery system between the battery, transmitter and charger during the charging process will be investigated.

Chapter 2

Theory

In this chapter the theoretical basis which is used to describe the physics behind quantum batteries is discussed. First some mathematical definitions will be introduced in section 2.1. In section 2.2 these mathematical definitions will be used to describe the physics behind quantum batteries.

2.1. Formalism

The mathematical formalism which is used in this thesis, is defined as in *Griffiths* [4].

2.1.1. Spin-particles in the Hilbert space

The Hilbert space is a complete inner product space. One example of a Hilbert space is the vector space of square-integrable functions. In quantum mechanics the state of a physical system is represented by a vector in this vector space. The space for a spin-1/2 particle has two basis states. One is called spin down $|\downarrow\rangle$, and the other is called spin up $|\uparrow\rangle$. These basis states can be represented by spinors:

$$|\uparrow\rangle \equiv \begin{pmatrix} 1 \\ 0 \end{pmatrix}, \quad |\downarrow\rangle \equiv \begin{pmatrix} 0 \\ 1 \end{pmatrix}, \tag{2.1.1}$$

Multiple 1/2-spin particles, where all N particles are in the spin up state, can be represented by $|\uparrow, \cdots, \uparrow_N\rangle$. The Dicke model describes a collection of spins interacting with a cavity field mode. In this thesis this basis is used. N spin-1/2 particles with m spins up can be described by a Dicke state (see *Liu 2021* eq. 2, [6]):

$$|m\rangle_N = \frac{1}{\sqrt{\binom{N}{m}}} \sum_k P_k(|\uparrow, \cdots, \uparrow_m, \downarrow_{m+1}, \cdots, \downarrow_N\rangle), \tag{2.1.2}$$

where $\binom{N}{m} = N!/[m!(N-m)!]$ and P_k denotes the complete set of all possible distinct permutations of the spin particles.

2.1.2. Spin matrices

Single $1/2$-spin particle

For one 1/2-spin particle the state can be described by the Pauli-spin matrices. The Pauli-spin matrices are unitary and hermitian matrices, given by

$$\sigma^x = \begin{pmatrix} 0 & 1 \\ 1 & 0 \end{pmatrix}, \quad \sigma^y = \begin{pmatrix} 0 & -i \\ i & 0 \end{pmatrix}, \quad \sigma^z = \begin{pmatrix} 1 & 0 \\ 0 & -1 \end{pmatrix}, \tag{2.1.3}$$

where each matrix σ^j represents the observable corresponding to spin state along the j-axis. The σ^z eigenstates are given in (2.1.1).

The creation and annihilation operators are given by

$$\sigma^+ = \begin{pmatrix} 0 & 1 \\ 0 & 0 \end{pmatrix}, \quad \sigma^- = \begin{pmatrix} 0 & 0 \\ 1 & 0 \end{pmatrix}, \tag{2.1.4}$$

such that $\sigma^+|\downarrow\rangle = |\uparrow\rangle$ and $\sigma^-|\uparrow\rangle = |\downarrow\rangle$, where $|\uparrow\rangle$ and $|\downarrow\rangle$ are the spin eigenstates (2.1.1).

Multiple $1/2$-spin particles

For N 1/2-spin particles with m 1/2-particles up we have the total spin operator S^α, given by

$$S^\alpha = \sum_{i=1}^{N} \sigma_i^\alpha \qquad \alpha = x, y, z, \tag{2.1.5}$$

where σ_i^α represents the Pauli-spin matrix (2.1.3) for the α-axis for the i^{th} spin particle. The total spin ladder operators for N 1/2-spin particles are given by

$$S^\pm = S^x \pm iS^y, \tag{2.1.6}$$

These operators are defined such that, with m particles in the spin up state, one has

$$S^z |m\rangle_N \equiv (m - \frac{N}{2}) |m\rangle_N , \tag{2.1.7}$$

$$\begin{aligned} S^+|m\rangle_N &= \sqrt{\frac{N}{2}(\frac{N}{2}+1) - (m-\frac{N}{2})(m-\frac{N}{2}+1)}|m+1\rangle_N, \\ S^-|m\rangle_N &= \sqrt{\frac{N}{2}(\frac{N}{2}+1) - (m-\frac{N}{2})(m-\frac{N}{2}-1)}|m-1\rangle_N, \end{aligned} \tag{2.1.8}$$

$$\begin{aligned} S^+|N\rangle_N &= 0, \\ S^-|0\rangle_N &= 0, \end{aligned} \tag{2.1.9}$$

where $|m\rangle_N$ and $|m \pm 1\rangle_N$ are expressed as Dicke states (2.1.2). S^+ increments the number of quanta in a certain state, and S^- decrements the number of quanta by one in a certain state. Equations (2.1.7) and (2.1.8) look a bit different than in *Griffiths* (Ch.4.4, [4]). The reason for this is because in this thesis N and m are defined as the total number of particles and the number of particles in the up spin state, instead of the total spin.

2.1.3. Tensor product

The tensor product is a mathematical operation that combines two vectors or matrices to form a larger composite vector or matrix. For two matrices A and B, their tensor product $A \otimes B$ is defined as follows:

$$A \otimes B = \begin{pmatrix} a_{11}B & a_{12}B & \cdots & a_{1n}B \\ a_{21}B & a_{22}B & \cdots & a_{2n}B \\ \vdots & \vdots & \ddots & \vdots \\ a_{m1}B & a_{m2}B & \cdots & a_{mn}B \end{pmatrix}, \tag{2.1.10}$$

where A is an $m \times n$ matrix or vector and B is a $p \times q$ matrix or vector. The resulting tensor product is an $(mp) \times (nq)$ matrix or vector.

The tensor product of two quantum states $|\psi\rangle$ and $|\phi\rangle$ is given by

$$|\psi\rangle \otimes |\phi\rangle = \begin{pmatrix} \psi_1|\phi\rangle \\ \vdots \\ \psi_n|\phi\rangle \end{pmatrix}. \tag{2.1.11}$$

Take for example the state of N 1/2-spin particles each in the up state. It is represented by a tensor product between individual 1/2-spin states (2.1.1), given by

$$|\uparrow, \cdots, \uparrow_N\rangle = |\uparrow\rangle \otimes \cdots \otimes |\uparrow\rangle_N. \tag{2.1.12}$$

2.1.4. Density matrices

The density matrix, denoted by ρ, represents a mixed state of a quantum system:

$$\rho = \sum_i p_i |\psi_i\rangle\langle\psi_i|, \tag{2.1.13}$$

where p_i is the probability of the system being in a pure state $|\psi_i\rangle$. ρ is hermitian, pos-semidefinite and normalized such that Tr $[\rho] = 1$.

The trace of a square matrix M, denoted by Tr$[M]$, is defined as the sum of its diagonal elements:

$$\text{Tr}[M] = \sum_i M_{ii}. \tag{2.1.14}$$

The expected value of an observable K can be calculated using the trace of the product of the observable and the density matrix describing the system:

$$\langle K \rangle = \text{Tr}[\rho K] = \sum_i p_i \langle\psi_i|K|\psi_i\rangle, \tag{2.1.15}$$

where ρ is the density matrix.

If ρ_Ω is the density matrix representing the state of a quantum system $\Omega = \Theta \otimes \Lambda$, where $\otimes$ is the tensor product (2.1.10) and Θ and Λ are the subsystems, the reduced density matrix representing the state of subsystem Λ is given by

$$\rho_\Lambda = \text{Tr}_\Theta[\rho_\Omega], \tag{2.1.16}$$

2.1.5. Entanglement

To give a characterization to the entropy entanglement for a subsystem Λ the Von Neumann entropy is used, given by

$$S(\rho_A) = -\mathrm{Tr}[\rho_\Lambda \log(\rho_\Lambda)] = -\sum_i p_{i_\Lambda} \log(p_{i_\Lambda}), \tag{2.1.17}$$

where ρ_Λ is the reduced density operator of a subsystem Λ at time t (2.1.16). $S(\rho_\Lambda)$ is zero if and only if ρ_Λ is a pure state. $S(\rho_\Lambda)$ is maximally equal to $\log N$ for a maximally mixed state, where N is the dimension of the Hilbert space.

2.1.6. Time evolution of a quantum system

The time-dependent Schrödinger equation describes the evolution of a quantum state over time. It can be written as

$$i\hbar \frac{d}{dt}|\psi(t)\rangle = H|\psi(t)\rangle, \tag{2.1.18}$$

where $|\psi(t)\rangle$ is the quantum state, H is the Hamiltonian, and $\hbar$ is the reduced Planck's constant (in this thesis $\hbar = 1$).

If we have a closed system (no interaction with the environment), the Schrödinger equation can be written as the Von Neumann equation, given by

$$\frac{d}{dt}\rho(t) = -\frac{i}{\hbar}[H, \rho(t)], \tag{2.1.19}$$

where ρ is the density matrix representing the system (2.1.13) and H is the Hamiltonian of the system. The term on the right-hand side represents the unitary evolution governed by the commutator $[H, \rho]$.

2.2. Quantum battery physics

In this section the physics behind the central-spin quantum battery and the central-spin transmitter quantum battery will be discussed.

2.2.1. Central-spin quantum battery

The central-spin quantum battery (CS-battery) consists of N_B spin-1/2 particles in a magnetic field and is described by the Hamiltonian

$$H_B = B_z S^z_{N_B}, \tag{2.2.1}$$

where B_z is the magnetic field applied along the z-axis and $S^z_{N_B}$ is the total spin operator (2.1.5) for N_B battery cells.

The charger consists of N_C spin-1/2 particles in a magnetic field and is described by the Hamiltonian

$$H_C = hS^z_{N_C}, \tag{2.2.2}$$

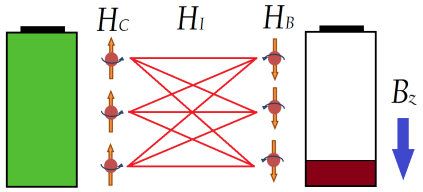

Figure 2.1: Schematic illustration of the CS-battery system with an magnetic field B_z applied in the downward direction. On the left there are N_C particles in the spins up state serving as charging cells, described by H_C. On the right there are N_B particles in the spins down state (ground state) serving as battery cells, described by H_B. The red lines between represent the interaction between the charger and battery cells, described by H_I.

where h is a constant and represents the energy stored in a single charger spin in the excited state and $S^z_{N_c}$ is the total spin operator (2.1.5) for N_C charger cells. Throughout the evaluation of the CS-battery, the paramters B_z and h are set as $B_z = h = 1$.

The exchange coupling between the battery and charger is given by the Hamiltonian

$$H_I = A\left(S^+_{N_B} J^-_{N_C} + S^-_{N_B} J^+_{N_C}\right) + \Delta S^z_{N_B} J^z_{N_C}, \tag{2.2.3}$$

where $S^\alpha_{N_B}$ and $J^\alpha_{N_C}$ (with $\alpha = +, -, z$) are the total spin operators (2.1.6) and (2.1.5). $S^\alpha_{N_B}$ works on the battery cells, $J^\alpha_{N_C}$ works on the charger cells (J is chosen instead of S to be clearer that this operator works on the charger cells and not on the battery cells). The parameter A and Δ characterize the flip-flop interaction and the Ising interaction respectively. These are set to $A = 1$ and $\Delta = 0$ throughout the evaluation of the CS-battery.

The total Hamiltonian of the battery-charger system is then given by

$$H_{tot} = H_B + H_C + H_I. \tag{2.2.4}$$

In Figure 2.1 there is a schematic illustration of the CS-battery system, where the charger is fully charged and the battery empty.

2.2.2. Central-spin transmitter quantum battery

Now instead of coupling between the battery and charger spins particles directly, there is a transmitter spin particle placed between the battery and charger spins. In this thesis it is called the central-spin transmitter quantum battery (CST-battery). To illustrate this, there is a schematic illustration in Figure 2.2. The Hamiltonian to describe this system is given by

$$H_{tot} = H_B + H_{I_1} + H_T + H_{I_2} + H_C, \tag{2.2.5}$$

where H_B and H_C are as described in Equations (2.2.1) and (2.2.2) respectively. H_T is the Hamiltonian of the transmitter spin given by

$$H_T = DS^z_{N_T}, \tag{2.2.6}$$

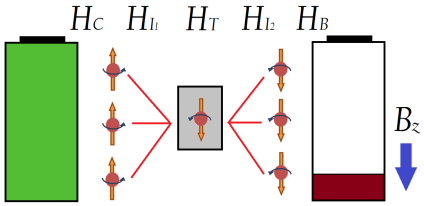

Figure 2.2: Schematic illustration of the CST-battery with an magnetic field B_z applied in the downward direction. On the left we have N_C particles in the spins up state serving as charger cells, described by H_C. In the middle we have one spin down (ground state) serving as transmitter cell, described by H_T. On the right we have N_B particles in the spins down state (ground state) serving as charger cells, described by H_C. The red lines on the left, between the charger cells and the transmitter cell, represent the interaction between the charger and transmitter cell, described by H_{I_1}. The red lines on the right, between the transmitter cell and the battery cells, represent the interaction between the transmitter cell and the battery cells, described by H_{I_2}.

Where D is a constant and represents the energy stored in a single charger spin in the excited stat and $S^z_{N_T}$ is the total spin operator (2.1.5) for N_T transmitter cells. Throughout the evaluation of the CST-battery, $N_T = 1$.

The parameters B_z, h and D are set as $B_z = h = D = 1$ throughout the evaluation of the CST-battery.

T he exchange coupling between the battery and the transmitter is described by H_{I_1}, which is given by

$$H_{I_1} = A_1 \left(S^+_{N_B} J^-_{N_T} + S^-_{N_B} J^+_{N_T} \right) + \Delta_1 S^z_{N_B} J^z_{N_T}, \tag{2.2.7}$$

where $S^\alpha_{N_B}$ and $J^\alpha_{N_T}$ with $(\alpha = +, -, z)$ are the total spin operators (2.1.6) and (2.1.5). $S^\alpha_{N_B}$ works on the battery cells, $J^\alpha_{N_T}$ works on the transmitter cell. The parameter A_1 and Δ_1 characterize the flip-flop interaction and the Ising interaction respectively.

H_{I_2} describes the exchange coupling between the transmitter and charger, which is given by the

$$H_{I_2} = A_2 \left(S^+_{N_C} J^-_{N_T} + S^-_{N_C} J^+_{N_T} \right) + \Delta_2 S^z_{N_C} J^z_{N_T}, \tag{2.2.8}$$

where $S^\alpha_{N_C}$ and $J^\alpha_{N_T}$ with $(\alpha = +, -, z)$ are the total spin operators (2.1.6) and (2.1.5). $S^\alpha_{N_C}$ works on the charger cells, $J^\alpha_{N_T}$ works on the transmitter cell. The parameter A_2 and Δ_2 characterize the flip-flop interaction and the Ising interaction respectively.

In both H_{I_1} and H_{I_2}, the parameters representing the strength of the Ising interaction are set to $\Delta_1 = \Delta_2 = 0$ throughout the evaluation of the CST-battery. The parameters representing the strength of the flip-flop interaction will be $A_1, A_2 \in \{0, 1\}$, which will enable/disable the exchange interaction. More information about determining the value of A_1 and A_2 will follow in section 3.2.2.

2.2.3. Energy, extractable work and charging power

The energy $E(t)$ stored in a quantum (sub)system at time t is given by

$$E_\Omega(t) = \langle E_\Omega(t) \rangle = \mathrm{Tr}\left[H_\Omega \rho_\Omega(t)\right], \tag{2.2.9}$$

where $\rho_\Omega(t)$ denotes the reduced density matrix of (sub-)system Ω, Tr[...] is the trace of the matrix (2.1.14) and $\langle ... \rangle$ denotes the expected value of an observable (2.1.15).

The maximum energy capacity a quantum battery can store, is given by

$$C_{E_B} = \mathrm{Tr}[H_B \rho_B^{\max}], \tag{2.2.10}$$

where $\rho_B^{\max} = |N_B\rangle_{N_B}\langle N_B|_{N_B}$. So if H_B and N_B stay constant, C_{E_B} stays constant.

The extractable work $W(t)$ stored in the quantum battery at time t is given by

$$W(t) = \mathrm{Tr}\left[H_B \rho_B(t)\right] - \mathrm{Tr}\left[H_B \tilde{\rho}_B(t)\right], \tag{2.2.11}$$

where $\tilde{\rho}_B(t)$ denotes the reduced density matrix of the passive state of the quantum battery. The passive state is defined as

$$\tilde{\rho}_B(t) = \sum_i^{N_B} r_i |\epsilon_i\rangle\langle\epsilon_i|, \tag{2.2.12}$$

where the eigenstates of $H_B = \sum_i^{N_B} \epsilon_i |\epsilon_i\rangle\langle\epsilon_i|$ and $\rho_B(t) = \sum_i^{N_B} r_i |r_i\rangle\langle r_i|$ are reordered so that $r_0 \geq r_1 \geq r_2 \geq \ldots$ and $\epsilon_0 \leq \epsilon_1 \leq \epsilon_2 \leq \ldots$. Passive states are defined as states that do not allow for work extraction in a cyclic (unitary) process. see also Eq. (3) in [10], and for more information about maximal work extraction, see [2, 1].

The charging power $P(t)$ of the battery is defined as the time-average of the energy that is stored in the battery at time t, given by

$$P_B(t) = (E_B(t) - E_B(0))/t, \tag{2.2.13}$$

where $E_B(t)$ and $E_B(0)$ are the energy and initial energy of the battery (2.2.9).

Chapter 3

Solutions for quantum batteries

In this chapter analytical and numerical results for for the time evolution of the energy E in the CS-battery and CST-battery are presented. For all solutions the parameters are kept $B_z = h = \hbar = 1$, where B_z and h represent the parameters described in (2.2.1) and (2.2.2) and $\hbar$ is the reduced Planck constant. The time is scaled by $t_{\text{scale}} = 1/B_z$. In section 3.1 the charging process CS-battery is studied analytically and numerically. In section 3.2 the charging process of the CST-battery is studied. Two types of setups are investigated for the CST-battery: one with a constant exchange coupling, and the other where the exchange coupling is modified during the charging process, where the exchange coupling is described by (2.2.7) and (2.2.8). Finally, at the end of this chapter, results regarding the total charging time T and average charging power P of the CST-battery are provided.

3.1. Central-spin battery

Before the charging process of the CS-battery is evaluated, the initial state of this closed system is determined. The battery is initialized with all spin particles in the spin down state $|0\rangle_{N_B}$ (the ground state). The charger is initialized with all spin particles in the spin up state $|m\rangle_{N_C}$, with $m = N_C$ (maximal excited state). Both the battery and charger are expressed in terms of the Dicke basis (2.1.2). The states collectively form the initial state of the system at time $t = 0$, given by

$$|\psi_0\rangle = |0\rangle_{N_B} \otimes |m\rangle_{N_C}\,, \tag{3.1.1}$$

where $\otimes$ is the tensor product (2.1.11).

The Hamiltonian which describes this system is given by (2.2.4). In terms of the Dicke basis equation (2.1.2), it can be represented as a reduced $(N_B + 1) \times (N_B + 1)$

matrix:

$$H = \begin{pmatrix} b_0 & u_1 & & & \\ u_1 & b_1 & u_2 & & \\ & \ddots & \ddots & \ddots & \\ & & u_{Nb-1} & b_{Nb-1} & u_{Nb} \\ & & & u_{Nb} & b_{Nb} \end{pmatrix}, \tag{3.1.2}$$

where the matrix components, are given by

$$\begin{aligned} u_j &= A\sqrt{j(N_B - j + 1)(N_C - m + j)(m - j + 1)}, \\ b_j &= B_z(j - \frac{N_B}{2}) + h(m - j - \frac{N_C}{2}) + 2\Delta(j - \frac{N_B}{2})(m - j - \frac{N_C}{2}), \end{aligned} \tag{3.1.3}$$

which are derived using Equations (2.1.7) and (2.1.8). This representation is the same as in *Liu 2021* (Eq. 10, [6]).

The Von Neumann equation (2.1.19) is used to evaluate the charging process of the CS-battery. In the library QuTip for Python [5], the function is implemented as *qutip.mesolve()*. In this case the Hamiltonian (3.1.2) is time-independent, so the Von Neumann equation can be solved to yield

$$\rho(t) = U(t)\rho_0 U^\dagger(t) \tag{3.1.4}$$

where $\rho_0 = |\psi_0\rangle\langle\psi_0|$ is the density matrix of the initial state (3.1.1), and $U(t) = e^{-iHt}$ is called the evolution operator. The reduced density matrix (2.1.16) for the battery and charger are $\rho_B = \mathrm{Tr}_C[\rho]$ and $\rho_C = \mathrm{Tr}_B[\rho]$ respectively.

Suppose H is diagonalized by a unitary matrix U and D the diagonal matrix. Than the evolution operator can be written as

$$U(t) = Ve^{-iDt}V^\dagger \tag{3.1.5}$$

The energy of the battery and the charger at time t is calculated using (2.2.9). The degree of entanglement between the battery and the charger is calculated using the Von Neumann entropy (2.1.17). If the entropy is not equal to zero, the battery cannot be in maximal energy state. An explanation for this is that the battery is in maximum energy state when $|\psi\rangle = |N_B\rangle_{N_B} \otimes |0\rangle_{N_C}$. This means the battery is in an pure state, which implies that the entropy is equal to zero. This is also discussed in *Liu 2021* and *Allahverdyan 2004*, [6, 2].

All results are plotted for $t < \pi^2$. This time period is chosen based on the result that will be obtained in section 3.2.2. It will be shown that it is possible to fully charge a CST-battery for $t < \pi^2$. So, for comparison between the CS-battery and CST-battery, larger time periods larger than π^2 are unnecessary.

Special case $N_B = 1$

For the case $N_B = 1$ and $N_C \geqslant 1$, the energy of the battery E_B reaches the full energy capacity of the battery C_{E_B} in certain time. This can be concluded from the analytical proof in *Liu 2021* (B. [6]). For the case $N_B = 1$ and $N_C \geqslant 1$, the Hamiltonian in (3.1.2) is reduced to

$$H = \begin{pmatrix} b_0 & u_1 \\ u_1 & b_1 \end{pmatrix}, \tag{3.1.6}$$

where u_j and b_j are the same as the ones in (3.1.3).

Solving the evolution operator (3.1.5), the matrices D and V are given by $D = \text{diag}(e_1, e_2)$, with the eigenenergies

$$\begin{aligned} e_1 &= \frac{b_0 + b_1}{2} + \sqrt{u_1^2 + \frac{1}{4}(b_0 - b_1)^2}, \\ e_2 &= \frac{b_0 + b_1}{2} - \sqrt{u_1^2 + \frac{1}{4}(b_0 - b_1)^2}, \end{aligned} \tag{3.1.7}$$

and

$$V = \frac{1}{u_1}\begin{pmatrix} e_2 - b_1 & e_1 - b_1 \\ u_1 & u_1 \end{pmatrix}, \quad V^\dagger = \frac{1}{e_2 - e_1}\begin{pmatrix} u_1 & b_1 - e_1 \\ -u_1 & e_2 - b_1 \end{pmatrix}. \tag{3.1.8}$$

Now solving (3.1.4), with the initial state determined as in (3.1.1), the reduced density matrix for (2.1.16) (we don't have to take the partial trace because (3.1.2) is already the reduced Hamiltonian) is given by

$$\rho_B(t) = \begin{pmatrix} \frac{1-r(t)}{2} & 0 \\ 0 & \frac{1+r(t)}{2} \end{pmatrix}, \tag{3.1.9}$$

where

$$r(t) = \left(\frac{b_0 - b_1}{2e_1 - b_0 - b_1}\right)^2 + \cos((e_1 - e_2)t)\left(\frac{u_1}{e_1 - \frac{1}{2}b_0 - \frac{1}{2}b_1}\right)^2. \tag{3.1.10}$$

If $B_z = h$ and $\Delta = 0$, b_j is the same for all $0 \leq j \leq N_B$, and (3.1.9) reduces to

$$\rho_B(t) = \begin{pmatrix} \frac{1-\cos(\omega t)}{2} & 0 \\ 0 & \frac{1+\cos(\omega t)}{2} \end{pmatrix} = \frac{1 - \cos(\omega t)}{2}|1\rangle_{N_B}\langle 1|_{N_B} + \frac{1 + \cos(\omega t)}{2}|0\rangle_{N_B}\langle 0|_{N_B}, \tag{3.1.11}$$

where $\omega = e_1 - e_2 = 2u_1$, the highest energy eigenstate of the battery $|1\rangle_{N_B}$, and the lowest energy eigenstate of the battery $|0\rangle_{N_B}$, written in terms of the Dicke basis (2.1.2). So, the time to fully charge the one cell battery to maximum energy capacity C_{E_B}, is given by

$$\tau = \frac{\pi}{\omega} = \frac{\pi}{2u_1}. \tag{3.1.12}$$

In Figure 3.1 the case where $N_B = 1$ and $N_C = 5$ is plotted as an example. It can be observed that E_B indeed reaches C_{E_B} in the given time period, so the battery is fully charged, and that S is equal to zero at the times E_B is at maximum.

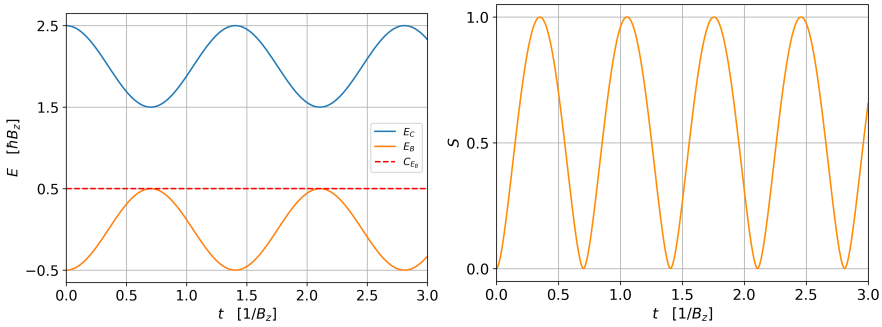

(a) Energy of CS-battery. $N_B = 1$, $N_C = 5$.

(b) Entropy of CS-battery. $N_B = 1$, $N_C = 5$.

Figure 3.1: The evolution of E and S for the CS-battery. The parameters are set as $N_B = 1$ and $N_C = 5$. The maximum energy capacity of the battery is $C_{E_B} = 0.5$. One can observe that E_B reaches C_{E_B} (the red dashed line) and that S is equal to zero at the times that E_B is at maximum.

Special case $N_B = 2$

For $N_B = 2$ and $N_C \geqslant 2$ it is not always the case that E_B reaches C_{E_B} in certain time. The Hamiltonian (3.1.2) reduces to

$$H = \begin{pmatrix} b_0 & u_1 & 0 \\ u_1 & b_1 & u_2 \\ 0 & u_2 & b_2 \end{pmatrix}, \tag{3.1.13}$$

where u_j and b_j are the same as the ones in (3.1.3).

If $\Delta = 0$ and $Bz = h$ and using the initial state determined as in (3.1.1), the eventual result for the evolution of ρ_B is given by

$$\rho_B(t) = \rho_{11}(t)|2\rangle_{N_B}\langle 2|_{N_B} + \rho_{22}(t)|1\rangle_{N_B}\langle 1|_{N_B} + \rho_{33}(t)|0\rangle_{N_B}\langle 0|_{N_B}, \tag{3.1.14}$$

where the highest energy eigenstate of the battery is $|2\rangle_{N_B}$, the second highest energy eigenstate of the battery is $|1\rangle_{N_B}$, and the lowest energy eigenstate of the battery is $|0\rangle_{N_B}$, written in terms of the Dicke basis (2.1.2). The occupation $\rho_{ii}(t)$ is given by

$$\begin{aligned} \rho_{11}(t) &= \frac{u_1^2 u_2^2}{(u_1^2 + u_2^2)^2}(1 - \cos(wt))^2, \\ \rho_{22}(t) &= \frac{u_1^2}{u_1^2 + u_2^2}(1 - \cos^2(wt)), \\ \rho_{33}(t) &= \frac{1}{(u_1^2 + u_2^2)^2}(u_2^2 + u_1^2\cos(wt))^2, \end{aligned} \tag{3.1.15}$$

with $\omega = e_2 - e_1 = \sqrt{u_1^2 + u_2^2}$.

The full derivation of this result can be found in *Liu 2021*, [6]. The occupation $\rho_{ii}(t)$ is plotted in figure 3.2e.

The occupation of the highest energy state of the battery is denoted by $\rho_{11}(t)$ (3.1.15). If $u_1 = u_2$, the occupation $p_{11}(t) = 1$ at time $t = \frac{\pi}{\omega}$. The battery is charged at maximal capacity C_{E_B}. This is the case if $N_C = N_B = 2$ and can be seen in Figure 3.2a. If $u_1 \neq u_2$, $\rho_{11}(t) < 1$ for all t, so the battery can never reach its maximum energy capacity C_{E_B}. This is the case if $N_C > N_B = 2$ and can be observed in Figure 3.2c. From Figure 3.2d and Figure 3.2e it can be observed that S is at highest value when the occupation of states is at most extensively distributed.

Arbitrary $N_B > 2$ case

For arbitrary $N_B, N_C > 2$, an analytical proof to show that E_B does not reach C_{E_B}, would be similar as for the cases $N_B = 1, 2$. But for $N_B = 3$, the reduced Hamiltonian (3.1.2) would be a 4×4 matrix. Calculating the eigenvalues (eigenenergies) and eigenvectors (eigenstates) would be long and complicated. Therefor, only results obtained from numerical simulations are shown for $N_B > 2$. In the appendix part of the code is given to make the Hamiltonian. In Figure 3.3, it holds true that for none of the cases E_B reaches C_{E_B} in $t < \pi^2$ time. Also, S is not equal to zero at the times that E_B is at it's maximum in. Even for the case $N_B = N_C = 100$, E_B does not reach C_{E_B} in $t < \pi^2$ (At its maximum, close to $t = 0$, $E_B < 49$). The initial states for the cases in Figure 3.3 are determined as in (3.1.1).

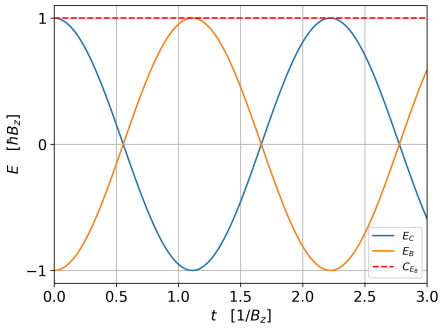

(a) Energy of CS-battery, $N_B = N_C = 2$.

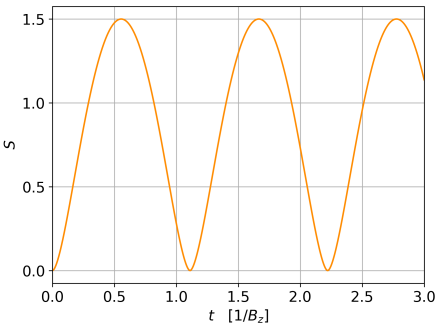

(b) Entropy of CS-battery, $N_B = N_C = 2$.

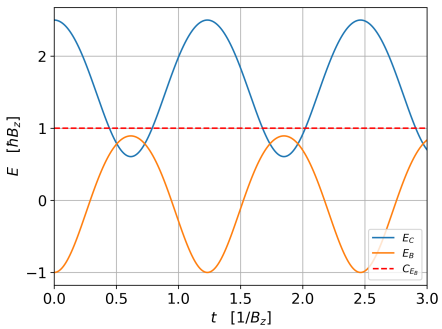

(c) Energy of CS-battery, $N_B = 2$ and $N_C = 5$.

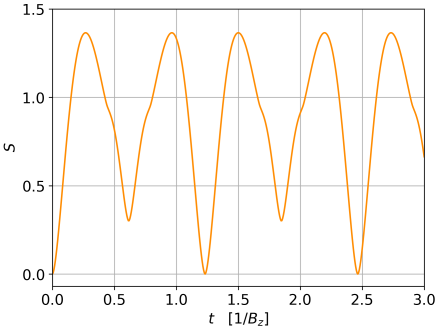

(d) Entropy of CS-battery, $N_B = 2$ and $N_C = 5$.

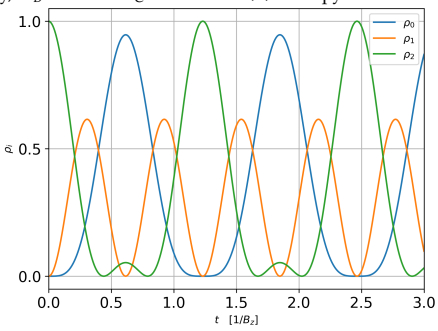

(e) Occupation of states, $N_B = 2$ and $N_C = 5$.

Figure 3.2: The evolution of E and S for the CS-battery. The occupation of the states (3.1.15), for the case $N_B = 2$ and $N_C = 5$, is shown in e. In a and b the parameters are set as $N_B = 2$ and $N_C = 2$. In c and d the parameters are set as $N_B = 2$ and $N_C = 5$. The initial states are determined as in (3.1.1). In both cases, $C_{E_B} = 1$. For $N_B = N_C = 2$ one can see that the battery is fully charged, and that S is equal to zero at the times that E_B is at maximum. This is not the case for $N_B = 2$ and $N_C = 5$. In d, one can see that S equals zero at multiple $t > 0$. This is because the charger is at full energy capacity C_{E_C} again, which is a pure state, which implies S is equal to zero. On the other hand S is maximal at the times that the occupation of states is most extensively distributed, as can be observed in e compared to d.

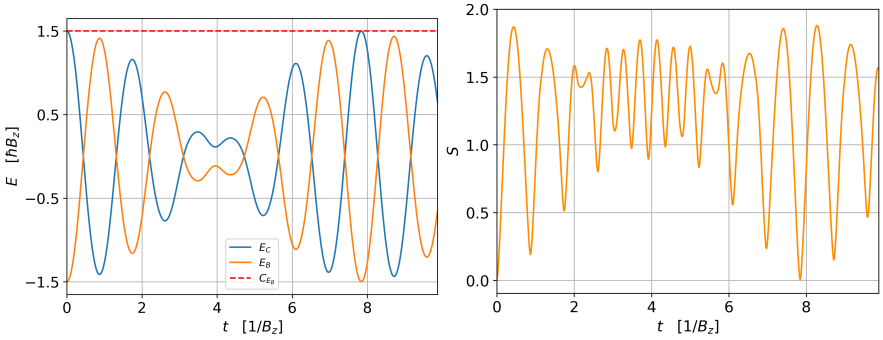

(a) Energy of CS-battery, $N_B = N_C = 3$.

(b) Entropy of CS-battery, $N_B = N_C = 3$.

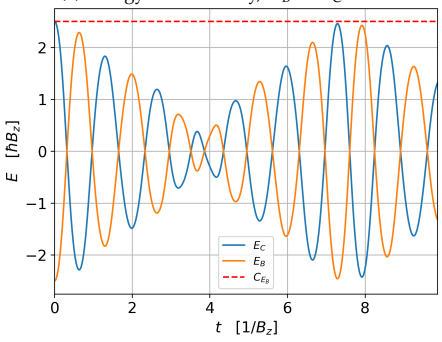

(c) Energy of CS-battery, $N_B = N_C = 5$.

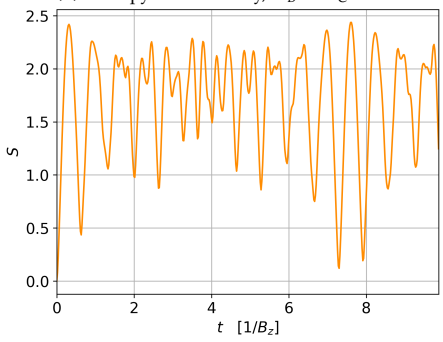

(d) Entropy of CS-battery, $N_B = N_C = 5$.

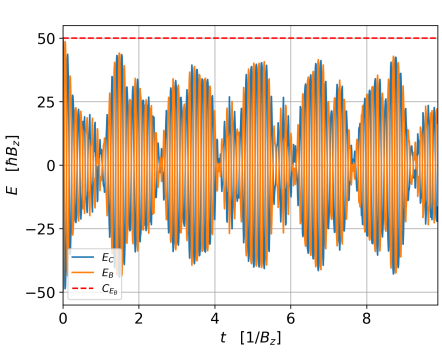

(e) Energy of CS-battery, $N_B = N_C = 100$.

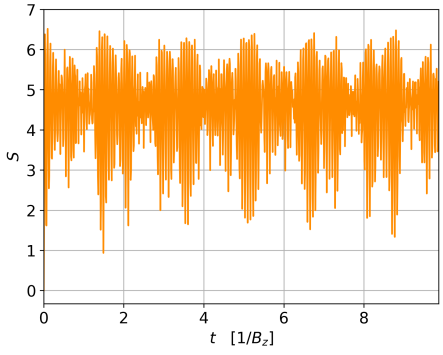

(f) Entropy of CS-battery, $N_B = N_C = 100$.

Figure 3.3: The evolution of the E and S of the CS-battery. In a and b the parameters are set as $N_B = N_C = 3$, with $C_{E_B} = 1.5$. In c and d the parameters are set as $N_B = N_C = 5$, with $C_{E_B} = 2.5$. In e and f the parameters are set as $N_B = N_C = 100$, with $C_{E_B} = 50$. One can see, that for all cases it is not possible to fully charge the battery in $t < \pi^2$ time. Also, S is never zeron for $t < \pi^2$, except around $t = 7.8$ in b, where the battery is empty, a pure state.

3.2. Central-spin transmitter battery

Now the charging process of the charging process of the CST-battery is investigated (see Figure 2.2, where the CST-battery system is in the initial state). The initial state of the CST-battery is determined in a similar way as for the CS-battery system: The battery and the transmitter are initialized with all spin particles in the spin down state $|0\rangle_{N_B}$ and $|0\rangle_{N_T}$, where N_T represents the number of spin particles in the transmitter, and in this case, it is equal to 1. The charger is initialized with all spin particles in the spin up state $|m\rangle_{N_C}$, with $m = N_C$. The battery, transmitter and charger are all three expressed in terms of the Dicke basis (2.1.2). These states collectively form the initial state of the system at time $t = 0$, given by

$$|\psi_0\rangle = |0\rangle_{N_B} \otimes |0\rangle_{N_T} \otimes |m\rangle_{N_C} \tag{3.2.1}$$

where $\otimes$ is the tensor product (2.1.11).

The Hamiltonian describing this system is given by (2.2.5). Two cases are investigated. In the first case, the exchange coupling H_{I_1} (2.2.7) and H_{I_2} (2.2.8) are kept constant. In the second case, the exchange coupling H_{I_1} and H_{I_2} are switched on and of alternately during the charging process by modifying the values of A_1 and A_2, where they can be equal to 0 or 1 (see Figure 3.6). The method of calculating the time interval between switching is explained in section 3.2.2.

3.2.1. Constant exchange coupling

If the exchange coupling H_{I_1} and H_{I_2} are kept constant with $A_1 = A_2 = 1$, the Hamiltonian describing this system (2.2.5), is time-independent. The Von Neumann equation than is solved in same manner as (3.1.4).

One can see in Figure 3.4 and Figure 3.5, that S_B and S_C seem to follow each other. This can be explained by the fact that the spins up/down are similarly distributed in the charger and battery. At time $t = 0$, the battery is empty and the charger is full, both in a pure state. At $t > 0$ the number of spins up in the batter and transmitter, will be exactly the number of spins down in the charger. So in the case of constant exchange coupling, if $N_B \approx N_C$ and N_T is relatively small in comparison with N_B and N_C, $S_B \approx S_C$. In Figure 3.5f, this is clearly visible.

Special case $N_B = 2$

For $N_B = 2$ and $N_C \geqslant 2$ the evolution of E and S is plotted in Figure 3.4. The initial states are determined as in (3.2.1). For both $N_C = 2$ and $N_C = 5$, it can be seen that E_B does not reaches C_{E_B} in $t < \pi^2$. Also, S is not equal to zero at the times E_B is at maximum.

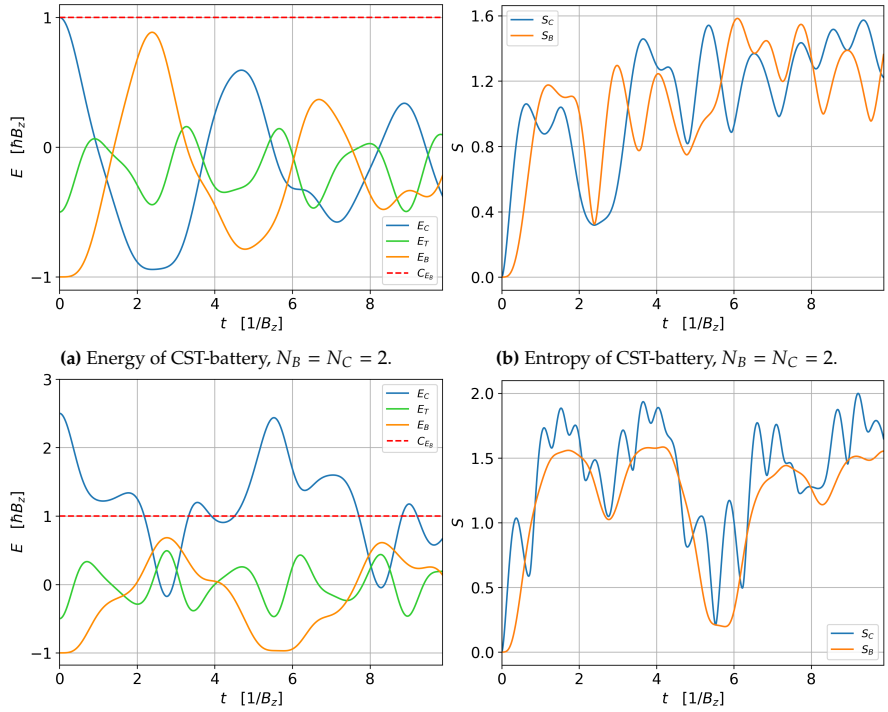

(a) Energy of CST-battery, $N_B = N_C = 2$.

(b) Entropy of CST-battery, $N_B = N_C = 2$.

(c) Energy of CST-battery, $N_B = 2$ and $N_C = 5$.

(d) Entropy of CST-battery, $N_B = 2$ and $N_C = 5$.

Figure 3.4: The evolution of the energy and entropy of the CST-battery, with $A_1 = A_2 = 1$ held constant. In a and b the parameters are set as $N_B = N_C = 2$. In c and d the parameters are set as $N_B = 2$ and $N_C = 5$. In both cases $C_{E_B} = 1$. For all cases, the battery is not fully charged in $t < \pi^2$ time. Also, S is not equal to zero at the times E_B is at maximum.

Arbitrary $N_B > 2$ case

For arbitrary $N_B, N_C > 2$ the evolution of E and S are plotted in Figure 3.5. For each case, E_B does not reach C_{E_B} in $t < pi^2$ time. Also, S is not equal to zero at the moments when E_B is maximal.

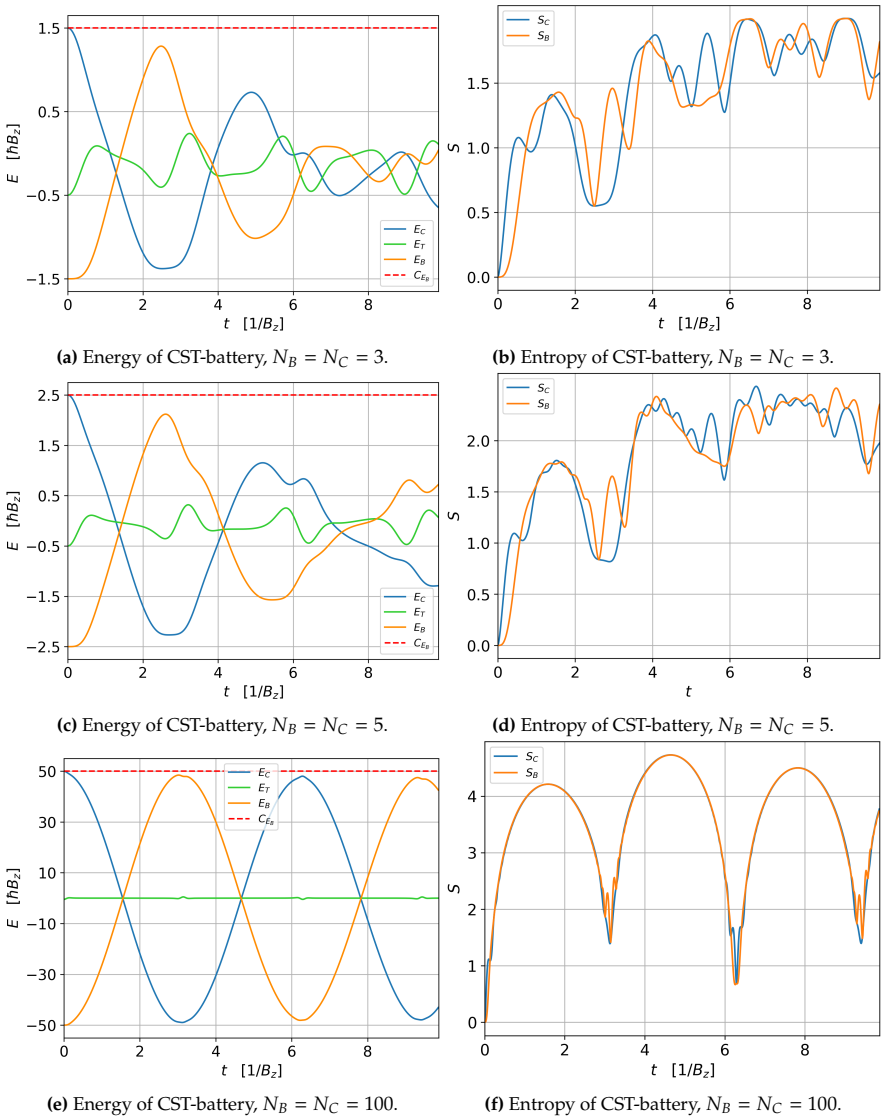

(a) Energy of CST-battery, $N_B = N_C = 3$.

(b) Entropy of CST-battery, $N_B = N_C = 3$.

(c) Energy of CST-battery, $N_B = N_C = 5$.

(d) Entropy of CST-battery, $N_B = N_C = 5$.

(e) Energy of CST-battery, $N_B = N_C = 100$.

(f) Entropy of CST-battery, $N_B = N_C = 100$.

Figure 3.5: The evolution of the energy and entropy of the CST-battery, with $A_1 = A_2 = 1$ held constant. In a and b the parameters are set as $N_B = N_C = 3$, with $C_{E_B} = 1.5$. In c and d the parameters are set as $N_B = N_C = 5$, with $C_{E_B} = 2.5$. In e and f the parameters are set as $N_B = N_C = 100$, with $C_{E_B} = 50$. For all cases, the battery is not fully charged in $t < \pi^2$ time. Also, S is not equal to zero at the moments E_B is at maximum.

3.2.2. Modifying exchange coupling

Now the exchange coupling H_{I_1} and H_{I_2} are modified during the charging process. The Hamiltonian (2.2.5) describing this system is time-dependent. Initially, we set $A_1 = 1$ and $A_2 = 0$, with the initial state $|\psi_0\rangle$ determined as in (3.2.1). At a certain point the exchange coupling is switched, so $A_1 = 0$ and $A_2 = 1$, disabling H_{I_1} and enabling H_{I_2}. The process of switching is illustrated in Figure 3.6, representing one cycle of the charging process. To fully charge the battery, a total of $2N_B$ cycles are required.

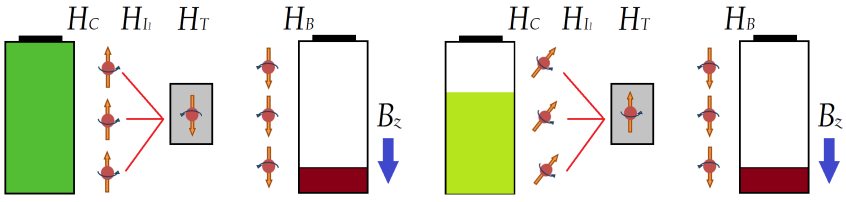

(a) The initial state of the CST-battery, at time $t = 0$.

(b) The transmitter is fully charged at $t = \tau_m$.

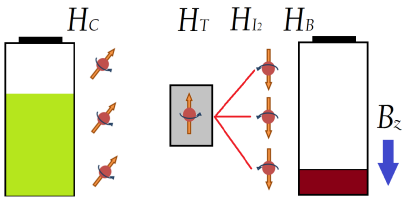

(c) The exchange coupling is switched at $t_0 = \tau_m$.

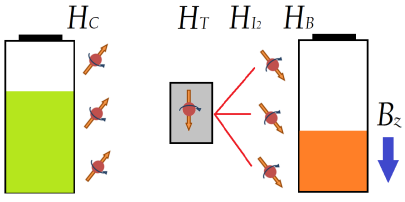

(d) The transmitter is fully discharged and has given all its energy to the battery, at $t = \tau_m + \tau'_{m_B}$.

Figure 3.6: An illustration of one cycle of the charging process of the CST-battery. In a, the CST-battery is in the initial state with $A_1 = 1$ and $A_2 = 0$. In b, the transmitter is fully charged ($E_T = C_{E_T}$) at $t = \tau_i$. In c, the exchange coupling is switched at $t = \tau_m$, so $A_1 = 0$ and $A_2 = 1$. In d the transmitter is fully discharged at $t = \tau_m + \tau_{m_B}$, and $E_B = C_{E_T}$. The tilted spins represent a superposition of up/down states (entangled state). To further charge the battery with $N_B > 1$, more cycles of switching are needed. The time interval τ_m and τ_{m_B} are calculated using (3.1.12).

The time interval between each switch is determined by the exchange coupling H_{I_1} or H_{I_2}. When only one exchange coupling operation is involved, the Hamiltonian (2.2.5) reduces to the Hamiltonian from (3.1.2), describing a CS-battery with $N_B = 1$. To understand why this is the case intuitively, one can compare the interaction between the charger-transmitter in Figure 3.6a with the interaction between the charger-battery in Figure 2.1, and observe their similarity. The transmitter reaches the energy level C_{E_T} in a time duration of τ_m, and fully discharges within a time duration of τ'_m, transferring all its energy to the battery. To calculate τ_m and τ'_m, the following equations are used:

$$\tau_m = \frac{\pi}{2u_m} = \frac{\pi}{2A_1\sqrt{(N_C - m + 1)m}}, \tag{3.2.2}$$

$$\tau'_{m_B} = \frac{\pi}{2u'_m} = \frac{\pi}{2A_2\sqrt{(N_B - m_B + 1)m_B}}, \tag{3.2.3}$$

where A_1 and A_2 are the parameters representing the strength of the exchange coupling, m the number of spin up particles in the charger and m_B the number of spin up particles in the battery. Equation (3.2.2) corresponds to (3.1.12), but in this case, the number of spin-up particles m/m_B in the charger/battery changes during the charging process. Therefore, m and m_B are used as a subscript instead of j (which is always equal to 1 because H is a 2×2 matrix). In Figure 3.7, the variation of τ_m with respect to the n-th cycle is plotted for the cases of $N_B = N_C = 5$ and $N_B = N_C = 100$.

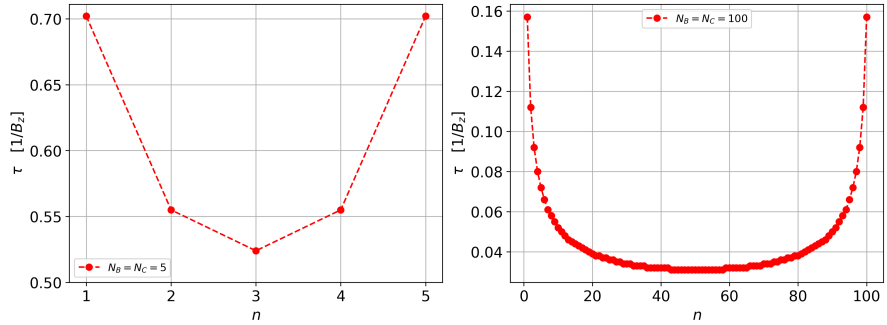

(a) $N_B = N_C = 5$.

(b) $N_B = N_C = 100$.

Figure 3.7: The time interval τ_m between each switch of the coupling between the battery-transmitter and transmitter-charger, for the n-th cycle of the charging process. In a, the parameters are set as $N_B = N_C = 5$. Five cycles of switching the coupling have to be performed to fully charge the battery. In b, the parameters are set as $N_B = N_C = 100$. To fully charge the battery, it requires hundred cycles of switching.

Now, between each switch, the Hamiltonian can be considered time-independent again, so the Von Neumann equation (2.1.19) can be solved in a similar way as how (3.1.4) is solved. As one can see in the following results, it is possible to fully charge the battery in $t < \pi^2$ for arbitrary $N_B \leq m \leq N_C$.

Special case $N_B = 2$ for comparison

For $N_B = 2$ and $N_C \geqslant 2$, the evolution of E and S is plotted in Figure 3.8. The initial states are determined as in 3.2.1. E_B reaches C_{E_B} in $t < \pi^2$ time. As needed, S_B and S_C are zero at the times or when the transmitter is fully charged or discharged.

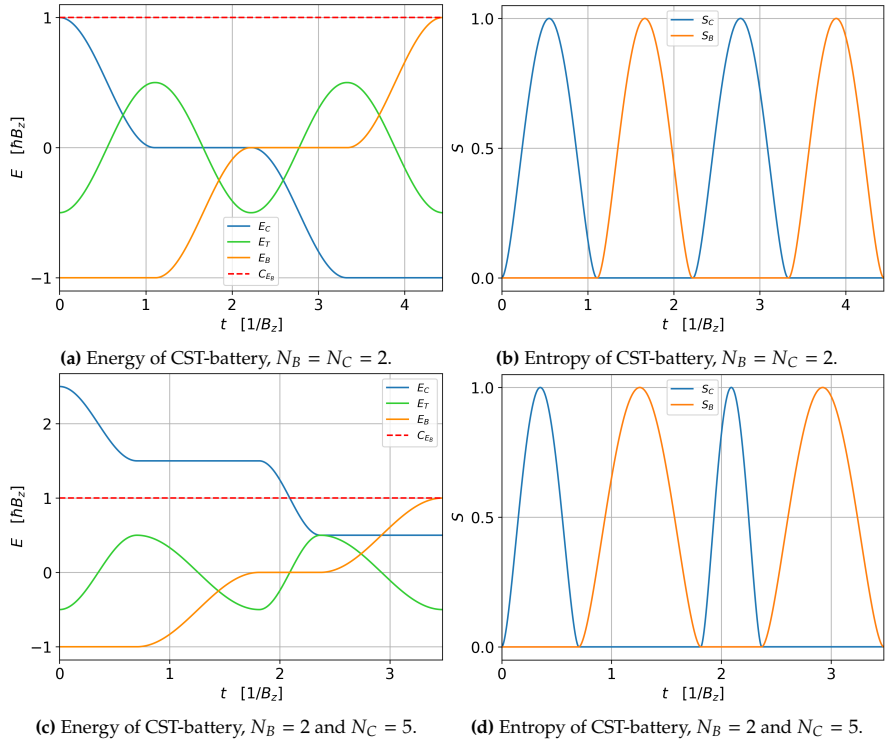

(a) Energy of CST-battery, $N_B = N_C = 2$.

(b) Entropy of CST-battery, $N_B = N_C = 2$.

(c) Energy of CST-battery, $N_B = 2$ and $N_C = 5$.

(d) Entropy of CST-battery, $N_B = 2$ and $N_C = 5$.

Figure 3.8: This is the evolution of the energy and entropy of the CST-battery, when Modifying switching H_{I_1} and H_{I_1} on and of alternately during the charging process. In a and b, the parameters are set as $N_B = N_C = 2$. In c and d, the parameters are set as $N_B = 2$ and $N_C = 5$. For both, $C_{E_B} = 1$. In both cases E_B reaches C_{E_B} in $t < \pi^2$ time, so the battery is fully charged. As needed, S_B and S_C are zero at the times or when the transmitter is fully charged or discharged.

Arbitrary $N_B > 2$ case for comparison

For arbitrary $N_B, N_C > 2$ the evolution of E and S are plotted in Figure 3.9. The initial states are determined as in 3.2.1. For each case, E_B reaches full energy capacity C_{E_B} in $t < \pi^2$ time. As needed, S_B and S_C are zero at the times E_T is fully charged, or fully discharged.

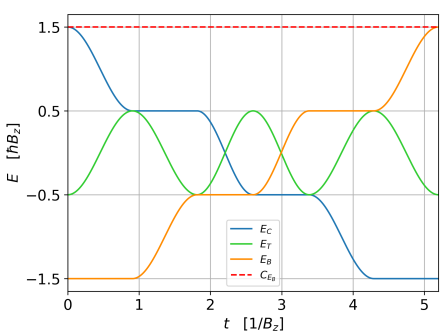

(a) Energy of CST-battery, $N_B = N_C = 3$.

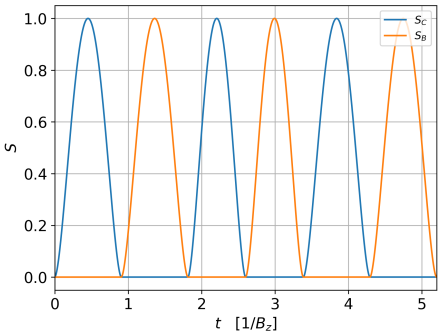

(b) Entropy of CST-battery, $N_B = N_C = 3$.

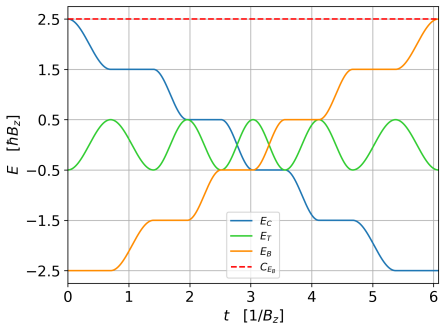

(c) Energy of CST-battery, $N_B = N_C = 5$.

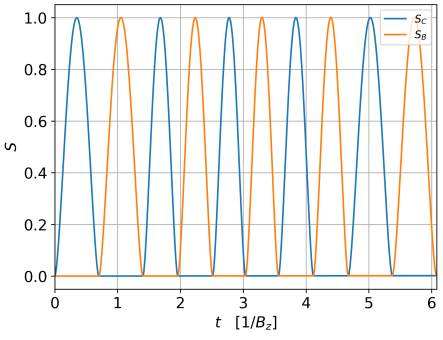

(d) Entropy of CST-battery, $N_B = N_C = 5$.

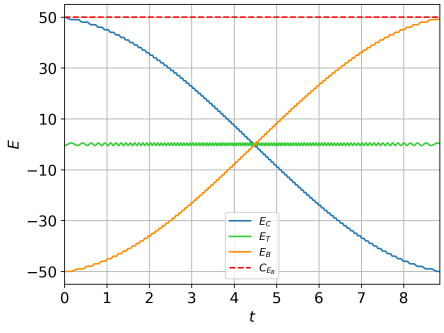

(e) Energy of CST-battery, $N_B = N_C = 100$.

Figure 3.9: The evolution of the energy and entropy of the CST-battery, when Modifying switching H_{I_1} and H_{I_1} on/of during the charging process. In a and b the parameters are set as $N_B = N_C = 3$, with $C_{E_B} = 1.5$. In c and d the parameters are set as N_B and $N_C = 5$, with $C_{E_B} = 2.5$. In e the parameters are set as $N_B = N_C = 100$, with $C_{E_B} = 50$. It may not be clearly visible, but also in e there are small oscillations. One can see that in all cases the battery is fully charged in $t < \pi^2$ time. As needed, S_B and S_C are zero at the times E_T is fully charged, or fully discharged.

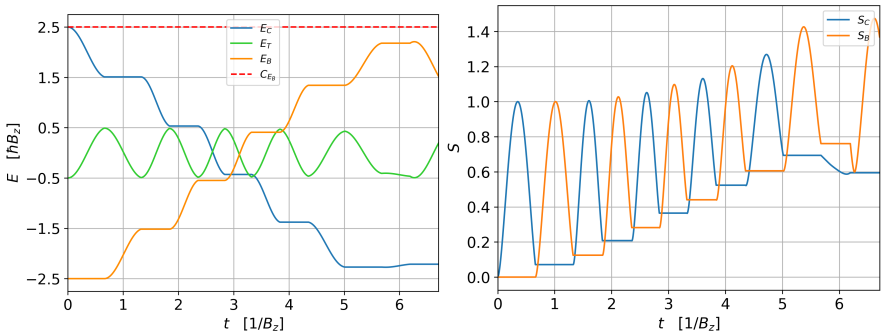

(a) Energy of CST-battery, $N_B = N_C = 5$.

(b) Entropy of CST-battery, $N_B = N_C = 5$.

Figure 3.10: The evolution of E and S of the CST-battery when switching the exchange coupling does not happen at a τ_m time interval after the previous switch. It can be seen that C_{E_B} is not reached, and that the average S increases, never equal to zero for $t > 0$. The subsystems stay entangled with each other.

Not switching at τ_m

In Figure 3.10 an example is given what happens when switching the exchange coupling does not happen at τ_m time after the previous switch, but at $\tau_m - 0.05$ for all m. The case $N_B = N_C = 5$ is plotted. One can see that E_B does not reaches C_{E_B}. In the end (around $t = 6$) the battery "leaks" energy back to the transmitter before it is fully charged. This happens because at the moment, the battery has relatively more energy than the transmitter. Also, the average S is increasing because at each switch particles between the subsystems stay entangled.

The convergence of total charging time for the CST-battery

The total time to fully charge the CST-battery if $N_C \geq m \geq N_B$, is given by

$$T = \sum_{1 \leqslant m \leqslant N_B} (\tau_m + \tau'_m) = \sum_{1 \leqslant m \leqslant N_B} \left(\frac{\pi}{2A_1\sqrt{(N_C - m + 1)m}} + \frac{\pi}{2A_2\sqrt{(N_B - m + 1)m}} \right), \tag{3.2.4}$$

where τ'_m and τ'_m are the times between each switch (3.2.2).

If N goes to infinity, the sum $\sum_{1 \leqslant x \leqslant N} 1/\sqrt{(N - x + 1)x}$ converges to π [1]. So, if N_B approaches infinity, the total charging time converges to

$$\lim_{N_B \to \infty} T = \lim_{N_B \to \infty} \sum_{1 \leqslant m \leqslant N_B} (\tau_m + \tau'_m) = \pi(\frac{\pi}{2} + \frac{\pi}{2}) = \pi^2 \tag{3.2.5}$$

This can be seen in Figure 3.11, where $N_B = N_C$.

[1] The sum $\sum_{1 \leqslant x \leqslant N} 1/\sqrt{(N - x + 1)x}$ is a Riemann integral if $N \to \infty$. The Riemann integral $\lim_{N \to \infty} \int_1^N 1/\sqrt{(N - x + 1)x} dx = \pi$

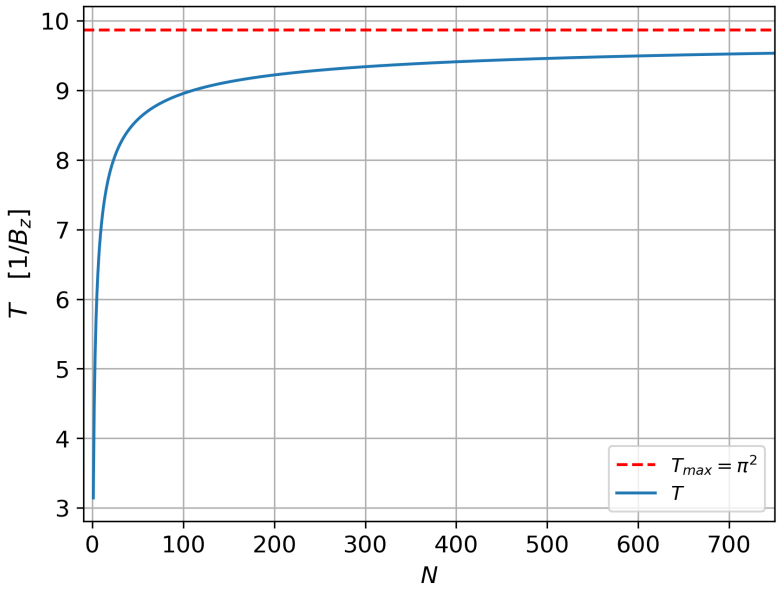

Figure 3.11: Time T to fully charge a battery, against the number of particles in the battery and charger $N_B = N_C$, where the initial state is determined as in (3.2.1). The time T to fully charge a battery, does not exceed π^2.

The power

Using (2.2.13) and (3.2.4), the average charging power P of the CST-battery is given by

$$P = \frac{2C_{E_B}}{T} = \frac{N_B}{\sum_{1 \leqslant m \leqslant N_B} (\tau_m + \tau'_m)} \tag{3.2.6}$$

where the average is calculated over the time it takes to fully charge the battery to its maximum energy capacity C_{E_B}.

For a CST-battery, if N_B approaches infinity, using (3.2.5), the average power becomes

$$\lim_{N_B \to \infty} P \sim \frac{N_B}{\pi^2} \tag{3.2.7}$$

Chapter 4

Discussion

In this chapter the analytically and numerically obtained results will be discussed and compared with existing literature. Also, suggestions for further research will be made.

Entanglement in the results
Entanglement is used to transfer energy from the charger to the battery in the central-spin quantum battery. Flip-flop interaction between the spin-particles is used to bring the particles in a superposition of ground and excited states. To be fully charged, the degree of entanglement needs to be zero again, because the quantum battery is in a pure state. Our results match the conclusions made in *Liu 2021* and *shi 2022*, [6, 10]: During the energy transition between two subsystems, the degree of entanglement between these subsystems first increases to the maximum which marks a nearly balanced distribution of occupation numbers, as can be observed in Figure 3.2d and Figure 3.2e. Thereafter, the degree entanglement decreases. Throughout this process the energy rises.

For the CST-battery, we have two possible combinations of subsystems available: The charger-transmitter and the transmitter-battery. If the exchange coupling remains constant for both subsystems, the degree of entanglement in each subsystem seems to be correlated. This correlation arises from the similarity in state occupation distribution between the subsystems, although with opposite energy states. This can be seen clearly in Figure 3.5f.

The CS-battery versus CST-battery
In this thesis, two distinct types of quantum batteries, namely the CS-battery and the newly introduced CST-battery, are investigated. In specific cases, such as $N_B = 1$, the battery in the CS-battery system can be fully charged. However, in most cases, the battery does not reach complete charging within $t < \pi^2$. On the other hand, by utilizing the transmitter as a lock and switching the exchanging coupling between the charger-transmitter and transmitter-battery alternately, it becomes possible to

fully charge the battery in the CST-battery system. This can even be analytically proven, because the mathematical description for this case is the same as for the CS-battery $N_B = 1$ case. When not switching after the correct time intervals τ_m (3.2.2), the battery cannot be fully charged. An example illustrating this is shown in Figure 3.10. Since the transmitter remains entangled with the charger/battery, the transmitter cannot be fully (dis)charged, resulting in the incomplete charging of the battery. It is likely that similar phenomena would occur in an experimental setup due to small errors in switching caused by the inability to instantaneously switch in zero time.

The average charging power of the CST-battery is proportional to $\frac{N_B}{\pi^2}$ as N_B approaches infinity, which is significantly lower than the upper bound of charging power for a CS-battery as derived in *Peng 2021* [9], given by $P_{\max} = 0.72BA\sqrt{N}N_B^{3/2}$. Here B, A, N and N_B are the parameters representing the magnetic field strength, the exchange coupling strength, the number of charger particles and the number of battery particles respectively, similar as in this thesis. This highlights that complete charging comes at the expense of fast charging.

Therefore, while the battery in the CST-battery system can be fully charged, the battery in the CS-battery system cannot always completely charged. On the other hand, the CS-battery charges a large portion of its total energy capacity relatively quickly compared to the CST-battery. Hence, the choice between the two depends on the specific requirements, where one may prioritize complete charging or fast charging.

Further research

There are multiple interesting paths to explore for further research. The papers *Liu 2021* and *Shi 2022* investigate the extractable work and the involvement of passive states [6, 10]. Passive states are defined as states that do not allow for work extraction in a cyclic (unitary) process. It would be interesting to examine the behavior of extractable work and passive states during the charging process of a CST-battery, considering that energy has a small "passage" through the transmitter.

The influence of energy dissipation on the CS-battery and CST-battery can also be studied. For instance, it is worth investigating what happens to the optimal time interval τ (3.2.2) when the transmitter dissipates energy into the environment. This information would be crucial for designing an experimental setup.

Another interesting aspect to consider is the exploration of the reasonable number of particles that can be entangled with each other and the method by which they can be brought into an entangled state. This analysis would provide insights into the maximum number of particles for which a quantum battery would still be feasible.

Chapter 5

Conclusion

In this thesis the role of entanglement and the optimal charging of central-spin quantum batteries is studied. Two types of systems were investigated: The CS-battery and the new CST-battery system.

The role of entanglement
The entanglement is characterized by the Von Neumann entropy. The exchange operator, which describes the flip-flop interaction between particles of the charger, transmitter and battery, is used to entangle particles between these subsystems with each other. This is needed to transfer the energy from one subsystem to the other. During the energy transition between two subsystems, the degree of entanglement between these subsystems is at maximum when the distribution of occupation numbers of possible states is most extensively distributed. For a subsystem to be in the maximal energy state (pure state), the degree of entanglement with another subsystem needs to be zero.

Central-spin battery
In section 3.1 analytical and numerical solutions are given for the evolution of energy and entanglement in a CS-battery. Special cases $N_B = 1$ and $N_B = 2$ are analytically solved. For $N_B = 1$ it is clear from the analytical and numerical results that the battery is fully charged when the degree of entanglement is equal to zero. The same goes for the case $N_B = N_C = 2$. If $N_C > N_B = 2$, it is analytically proven that the battery is never fully charged, and that the degree of entanglement is not equal to zero at the moments E_B is at its maximum. For $N_C, N_B > 2$ the numerical solutions show that the battery is also not fully charged in $t < \pi^2$ time. Also, the degree of entanglement is not equal to zero at the moments E_B is at its maximum, meaning the particles are entangled, so the particles cannot be in maximum energy state (pure state).

Central-spin transmitter battery

In section 3.2 the numerical solutions are given for the evolution of energy and entanglement in a CST-battery. If holding the exchange coupling constant, the battery again is not fully charged in $t < \pi^2$ time. On the other hand, by enabling and disabling the exchange coupling between the charger-transmitter and the transmitter-battery alternately, at precise moments, it is possible to fully charge the battery. The transmitter is used as a lock. When one of the exchange couplings between charger-transmitter or transmitter battery is disabled, the subsystem can be considered as a CS-battery, with only a 2×2 Hamiltonian (3.1.6). The total charging time T to fully charge a CST-battery can be calculated using Equation (3.2.4). If $N_B \leq m \leq N_C$, and N_B approaches infinity, the total charging time T converges to π^2. Finally, it can be concluded that the power $P \sim \frac{N_B}{\pi^2}$ as N_B approaches infinity.

Where the CS-battery can charge a substantial portion of its total energy capacity relatively quickly, it often falls short of reaching full energy capacity. In contrast, the CST-battery can theoretically achieve full energy capacity during the charging process.

References

[1] Robert Alicki and Mark Fannes. "Entanglement boost for extractable work from ensembles of quantum batteries". In: *Physical Review E* 87.4 (Apr. 2013). DOI: 10.1103/physreve.87.042123. URL: https://doi.org/10.1103%5C%2Fphysreve.87.042123.

[2] A. E. Allahverdyan, R. Balian, and Th. M. Nieuwenhuizen. "Maximal work extraction from finite quantum systems". In: *Europhysics Letters* 67.4 (Aug. 2004), p. 565. DOI: 10.1209/epl/i2004-10101-2. URL: https://dx.doi.org/10.1209/epl/i2004-10101-2.

[3] Felix C Binder et al. "Quantacell: powerful charging of quantum batteries". In: *New Journal of Physics* 17.7 (July 2015), p. 075015. DOI: 10.1088/1367-2630/17/7/075015. URL: https://doi.org/10.1088%5C%2F1367-2630%5C%2F17%5C%2F7%5C%2F075015.

[4] David J. Griffiths and Darrel F. Schroeter. *Introduction to Quantum Mechanics*. 3th ed. Cambridge, United Kingdom: Cambridge university press, 2018.

[5] J. R. Johansson, Paul D. Nation, and Franco Nori. "QuTiP: An open-source Python framework for the dynamics of open quantum systems." In: *Comput. Phys. Commun.* 183.8 (2012), pp. 1760–1772. URL: http://dblp.uni-trier.de/db/journals/cphysics/cphysics183.html#JohanssonNN12.

[6] Jia-Xuan Liu et al. "Entanglement and work extraction in the central-spin quantum battery". In: *Physical Review B* 104.24 (Dec. 2021). DOI: 10.1103/physrevb.104.245418. URL: https://doi.org/10.1103%5C%2Fphysrevb.104.245418.

[7] James Millen and André Xuereb. "Perspective on quantum thermodynamics". In: *New Journal of Physics* 18.1 (Jan. 2016), p. 011002. DOI: 10.1088/1367-2630/18/1/011002. URL: https://doi.org/10.1088%5C%2F1367-2630%5C%2F18%5C%2F1%5C%2F011002.

[8] James Millen and André Xuereb. "The rise of the quantum machines". In: *Physics World* 29 (2016), pp. 23–26.

[9] Li Peng et al. "Lower and upper bounds of quantum battery power in multiple central spin systems". In: *Physical Review A* 103.5 (May 2021). DOI: 10.1103/physreva.103.052220. URL: https://doi.org/10.11032Fphysreva.103.052220.

[10] Hai-Long Shi et al. “Entanglement, Coherence, and Extractable Work in Quantum Batteries”. In: *Physical Review Letters* 129.13 (Sept. 2022). DOI: 10.1103/physrevlett.129.130602. URL: https://doi.org/10.1103%5C%2Fphysrevlett.129.130602.

Appendix A

Source Code

This is part of my code to create the Hamiltonian's for the CS-battery and the CST-battery. For the Hamiltonian in the CS-basis is made use of the equation (10) in *Liu 2021,* [6]. The full code will be available at:

`https://github.com/Quirijn015/Optimal-charging-quantum-batteries.git`.

```
"""
The class for making the Hamiltonian which describes the CS-battery.
"""

class CS_QB_Dicke:

    def __init__(self,Nb=1,Nc=1,m=1,Bz=1,h=1,A=1,delta=1:

        self.Nb = Nb
        self.Nc = Nc
        self.N = self.Nb+self.Nc
        self.m = m
        self.B = Bz
        self.h = h
        self.A = A
        self.delta = delta

        self.H = self.create_H(self.Nb,self.Nc,self.h,self.B,self.delta,
            self.A,self.m,self.intern)

        self.Hb = qt.jmat(self.Nb/2, "z")
        self.Hb = qt.Qobj(np.flip(np.flip(self.Hb.full())[:min(self.m,self.
            Nb,self.Nc)+1,:min(self.m,self.Nb,self.Nc)+1]))

        self.Hc = qt.jmat(self.Nc/2, "z")
        self.Hc = qt.Qobj(self.Hc.full()[:min(self.m,self.Nc,self.Nb)+1,:
            min(self.m,self.Nc,self.Nb)+1])

    def create_H(self,Nb,Nc,h,B,delta,A,m):

        n = min(self.Nb,self.m)
```

```
29
30          j = np.arange(n+1)
31          j_u = j[1:len(j)]
32
33          b_list = (B*(j-Nb/2)+h*(m-j-Nc/2)+
34                    2*delta*(j-Nb/2)*(m-j-Nc/2))
35          u_list = A*np.sqrt(j_u*(Nb-j_u+1)*
36                             (Nc-m+j_u)*(m-j_u+1))
37
38          H = np.diag(b_list) + np.diag(u_list,k=1) + np.diag(u_list,k=-1)
39
40          H[np.isnan(H)] = 0
41
42          return qt.Qobj(H)
43
44  """
45  The class for making the Hamiltonian which describes the CST-battery.
46  """
47
48  class CST_QB_Dicke:
49
50      def __init__(self,Nb,Nt,Nc,m,Bz=1,h=1,A1=1,A2=1,delta=0):
51
52          self.Nc = Nc
53          self.Nt = Nt
54          self.Nb = Nb
55
56          self.A1 = A1
57          self.A2 = A2
58
59          self.m = m
60
61          self.Hc = qt.jmat(self.Nc/2,"z")
62          self.Ht = qt.jmat(self.Nt/2,"z")
63          self.Hb = qt.jmat(self.Nb/2,"z")
64
65          self.Hi1 = self.create_Hi(self.Nc,self.Nt)
66          self.Hi2 = self.create_Hi(self.Nt,self.Nb)
67
68          self.Hc_N,self.Ht_N,self.Hb_N,self.Hi1_N,self.Hi2_N = self.
                create_tensors()
69
70          self.H = self.Hc_N+self.A1*self.Hi1_N+self.Ht_N+self.A2*self.Hi2_N+
                self.Hb_N
71
72      def create_Hi(self,N_1,N_2):
73
74          Hi = qt.tensor(qt.jmat(N_1/2,"+"),qt.jmat(N_2/2,"-"))+qt.tensor(qt.
                jmat(N_1/2,"-"),qt.jmat(N_2/2,"+"))
75
76          return Hi
77
78      def create_tensors(self):
79
80          Hc_N = qt.tensor([self.Hc,qt.qeye(self.Nt+1),qt.qeye(self.Nb+1)])
81          Ht_N = qt.tensor([qt.qeye(self.Nc+1),self.Ht,qt.qeye(self.Nb+1)])
82          Hb_N = qt.tensor([qt.qeye(self.Nc+1),qt.qeye(self.Nt+1),self.Hb])
```

```
83
84          Hi1_N = qt.tensor(self.Hi1,qt.qeye(self.Nb+1))
85          Hi2_N = qt.tensor(qt.qeye(self.Nc+1),self.Hi2)
86
87          return Hc_N,Ht_N,Hb_N,Hi1_N,Hi2_N
```